Energy Transfer Dynamics in the Presence of Preferential Hydrogen Bonding: Collisions of Highly Vibrationally Excited Pyridine-h_5, -d_5, and -f_5 with Water†

Qingnan Liu, Daniel K. Havey, and Amy S. Mullin*

Department of Chemistry and Biochemistry, University of Maryland, College Park, Maryland 20742

Received: March 17, 2008; Revised Manuscript Received: May 23, 2008

The relaxation of highly vibrationally excited pyridine-h_5, pyridine-d_5, and pyridine-f_5 ($E \approx 38\,000$ cm^{-1}) through collisions with water was investigated by high resolution transient IR absorption spectroscopy to investigate how preferential hydrogen bonding interactions impacts the energy transfer dynamics. Nascent rotational and translational energy gain profiles for scattered $H_2O(000)$ molecules with $E_{rot} > 1000$ cm^{-1} are reported. $H_2O(000)$ molecules scattered from pyridine-h_5 and pyridine-d_5 have rotational distributions with $T_{rot} = 890$ K. Less rotational energy is found in $H_2O(000)$ scattered from pyridine-f_5 for which $T_{rot} = 530$ K. The recoil energy distributions are similar for the three donors with $T_{rel} = 400-700$ K. To explain the results, a torque-inducing mechanism is proposed that involves directed movement of water between σ and π-hydrogen bonding interactions with the pyridine donors. The experimental results are consistent with this mechanism, and with effects due to the state-density energy dependence of the highly excited donor molecules. Differences in vibrational mode frequencies of the hot donor molecules do not appear to explain the experimental results.

Introduction

Hydrogen bonding interactions are important in a wide array of disciplines ranging from biochemistry[1–3] to atmospheric chemistry.[4–6] Preferential hydrogen bonding of H_2O and its isotopes has been observed in interactions with aromatic molecules. Stable binary complexes of nitrogen-containing aromatics with water have local minima for both σ- and π-type hydrogen bonding. The interaction of a hydrogen atom on water and the nitrogen lone pair leads to σ-type hydrogen bonding. In π-type hydrogen bonding, both hydrogen atoms of water interact with the aromatic π cloud. Using microwave spectroscopy in a molecular beam, Caminati and co-workers observed an interesting isotope effect in σ-type complexes of pyrazine ($C_4H_4N_2$) and water. They saw evidence for the $C_4H_4N_2-$HOH and $C_4H_4N_2-$DOH configurations but found no evidence for the $C_4H_4N_2-$HOD conformer.[7] They attributed the selective formation of the $C_4H_4N_2$-DOH complex to a lower zero point energy relative to $C_4H_4N_2-$HOD. A related isotope effect has been observed in collisional energy transfer from highly vibrationally excited pyrazine ($E = 38\,000$ cm^{-1}) with H_2O and HOD.[8,9] High-resolution transient IR absorption studies show that both H_2O and HOD are scattered with relatively small amounts of translational energy but that H_2O is scattered with twice the rotational energy of HOD. Stronger interactions with the nitrogen lone pair will tend to reduce the amount of rotational energy in the scattered molecules.

Hydrogen bonding interactions of water with aromatic π-systems have also been observed and characterized.[10–15] Rotationally resolved molecular beam experiments by Suzuki et al.[15] established that benzene-water clusters have the hydrogen atoms of water positioned toward the π-electron cloud.[15] Matrix isolation studies by Engdahl and Nelander[16] as well as resonance ionization studies by Gotch and Zweir[17] showed that the two hydrogen atoms, when vibrationally averaged, are equivalent. When benzene is fluorinated, however, the large electronegativity of the fluorine atoms distorts the π-electron distribution and leaves the carbon atoms electron deficient. Alkorta, Rozas, and Elguero characterized the electrostatics and interaction energies of a series of small molecules hydrogen bonded to C_6H_6 and to C_6F_6.[11,12] They found that stable complexes form between electron-donating atoms and the π-cloud of C_6F_6 while C_6H_6 attracts electron-deficient atoms.[11,15] Danten, Tassaing, and Besnard performed ab initio calculations at the Hartree−Fock and Møller−Plesset-2 levels on complexes of $H_2O-C_6F_6$ and $H_2O-C_6H_6$.[10] They found that both complexes have similar binding energies of ~2 kcal/mol, but that the orientation of H_2O with respect to the aromatic ring is opposite in the two complexes.[10,15] For C_6H_6, water is oriented with its hydrogen atoms toward the π-electron cloud of the aromatic ring. When complexed with C_6F_6, water is in its most stable configuration with the oxygen lone pairs directed toward the ring. Experimental calorimetry studies by Wormald and Wurzberger support the calculations of Danten, Tassaing and Besnard with orientationally averaged binding energies of ~1.3 ± 0.1 kcal/mol for both the hydrogenated and fluorinated benzene−water complexes.[18]

Here we explore how collisional energy transfer dynamics are affected by the presence of preferential hydrogen bonding interactions between highly vibrationally excited donor molecules and water. In this study we focus on the large-ΔE collisions that scatter water into high energy rotational states (with $E_{rot} > 1000$ cm^{-1}) in single encounters. These collisions correspond to the high energy tail of the vibration-to-rotation/translation (V-RT) energy transfer pathway. The V-RT pathway is the primary means by which highly vibrationally excited molecules relax through collisions. We have characterized the nascent rotational and translational energy gain profiles of water molecules that scatter from a series of high energy donors that have different π-electron distributions. The donor molecules, pyridine-h_5 (C_5H_5N), pyridine-d_5 (C_5D_5N), and pyridine-f_5 (C_5F_5N), are initially prepared with $E \approx 38\,000$ cm^{-1} by pulsed UV excitation prior to collisions with water at 300 K. The

† Part of the "Stephen R. Leone Festschrift".

* To whom correspondence should be addressed.

10.1021/jp802326t CCC: $40.75
Published on Web 08/19/2008

appearance of individual quantum states of scattered H_2O is monitored using high-resolution transient IR absorption at $\lambda = 2.7\ \mu$m.

Previously, we reported on the large-ΔE collisions of highly vibrationally excited pyridine-h_5 with H_2O that lead to rotational and translational excitation of $H_2O(000)$.[19] A sensitive test of large-ΔE collisions between vibrationally hot molecules and a 300 K bath is the nascent rotational temperature, T_{rot}, of scattered bath molecules. Earlier studies on a series of pyridine-based donors have shown that T_{rot} for scattered $H_2O(000)$ molecules (with $E_{rot} > 1000\ cm^{-1}$) decreases systematically for donors that have larger size, more vibrational modes, and increased vibrational state density.[20] In the present work, the three pyridine donors have the same number of vibrational modes ($n = 27$), are of similar size, and can interact with water through both σ- and π-type hydrogen bonding interactions. However, the intermolecular potential energy surface for the fluorinated donor has a minimum with water in the opposite orientation. Under our experimental conditions, the presence of stable complexes is unlikely but differences in specific local electrostatic interactions may influence the energy transfer dynamics. Other differences among these donors are mode frequencies and state densities. We will consider how each affects the outcome of large-ΔE collisions.

In this study, we report the nascent energy gain profiles for a number of rotational states of $H_2O(000)$ with $E_{rot} > 1000\ cm^{-1}$ that result from collisions with highly vibrationally excited pyridine-h_5, pyridine-d_5 and pyridine-f_5, each with $E \approx 38\,000\ cm^{-1}$. The dynamics of large-$\Delta E$ collisions between pyridine-h_5 and H_2O have been investigated previously.[19] In the current study we have repeated measurements on pyridine-h_5:H_2O and performed new measurements on collisions of H_2O with pyridine-d_5 and pyridine-f_5 using a recently constructed high-resolution transient IR absorption spectrometer. Our new measurements show that the high energy tail of the scattered H_2O distribution is affected by the donor identity. The three donors impart roughly the same amount of translational energy through large-ΛE collisions but there are differences in the rotational distributions of the scattered water molecules. Water molecules scattered from pyridine-h_5 and -d_5 (with $E_{rot} > 1000\ cm^{-1}$) have essentially the same rotational distribution. When pyridine-f_5 is the donor however, the nascent rotational temperature of the scattered water decreases by nearly 40%. We discuss the implications of these results in terms of differences in donor:H_2O interactions, donor state density, and donor mode frequencies.

Experimental Section

The current study was performed on a high-resolution transient IR absorption spectrometer at the University of Maryland. A description of the original spectrometer has been given previously and the current instrument retains the same major components.[21] After absorption of a 266 nm photon from the fourth harmonic of a pulsed Nd:YAG laser (2 Hz, 5 ns pulse duration), pyridine-h_5, -d_5 and -f_5 undergo rapid radiationless decay to vibrationally excited states with $E = 37\,950$, 38 068, and 38 832 cm^{-1}, respectively.[22–25] The radiationless decay of pyridine-h_5 has near unity quantum yield with a lifetime of ~60 ps.[23] Pyridine-d_5 and pyridine-f_5 are expected to have similar quantum yields and radiationless decay lifetimes.[24,25] The 266 nm pump beam was propagated collinearly along a 3 m Pyrex collision cell with a continuous and tunable single-mode F-center laser operating at $\lambda \approx 2.7\ \mu$m with a resolution of $0.0003\ cm^{-1}$. The F-center laser probed H_2O rotational transitions within the (001)←(000) asymmetric stretch transition. A number of $H_2O(000)$ rotational states with energy between $E_{rot} = 1000$ and 1800 cm^{-1} were investigated.

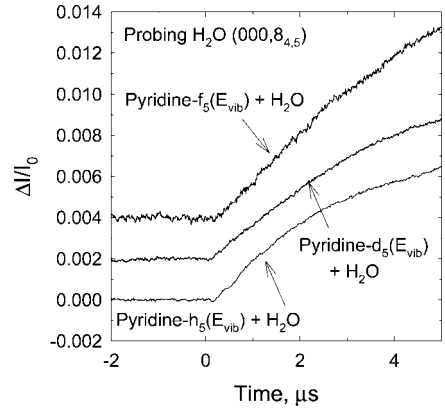

Figure 1. Fractional IR absorption of $H_2O(000,8_{4,5})$ following collisions of highly excited pyridine-h_5 ($E = 37\,950\ cm^{-1}$), pyridine-d_5 ($E = 38\,068\ cm^{-1}$), and pyridine-f_5 ($E = 38\,836\ cm^{-1}$) with H_2O measured at ν_0 as a function of time following UV excitation of the donor molecules. The transient absorption signal for $H_2O(000,8_{4,5})$ following collisions with highly excited pyridine-d_5 ($E = 38\,068\ cm^{-1}$) and pyridine-f_5 ($E = 38\,836\ cm^{-1}$) are offset by 0.002 and 0.004, respectively, for clarity.

Pyridine-h_5, -d_5, or -f_5 (Acros, 99+ %) and the vapor from HPLC grade $H_2O_{(l)}$ were introduced in a 1:1 mixture, with a total pressure ~25 mTorr, into the flowing gas collision cell. The total average cell pressure was determined using a spectroscopically calibrated manometer thereby accounting for the pressure gradient that exists in a flowing gas system, as described in Supporting Information. The UV intensity was kept less than 5 MW/cm^2 to minimize multiphoton absorption by the donor molecules. Under these conditions, the fraction of donor molecules that are photoexcited is 15% or less and the average time between collisions is ~2.5 μs.

$H_2O(000)$ molecules gain rotational and translational energy after single collisions with highly vibrationally excited donor molecules, as shown in eq 1.

$$\text{Donor(E)} + H_2O \xrightarrow{k_2^J} \text{Donor(E}') + H_2O(000, J_{KaKc'}V) \qquad (1)$$

The scattered $H_2O(000)$ molecules are described by the following: J, the total angular momentum; K_a and K_c, the components of the angular momentum along the A and C molecular axes, respectively; and V, the component of the velocity vector along the IR probe axis. k_2^J is the rate constant for the appearance of a single $J_{Ka,Kc}$ state of H_2O. IR probing of scattered $H_2O(000)$ molecules is described by eq 2.

$$H_2O(000, J_{KaKc}, V) + IR \rightarrow H_2O(001, J'_{Ka'Kc'}, V) \qquad (2)$$

Here $J'_{Ka'Kc'}$ are the quantum numbers for the upper state of the probe transition. The collisional relaxation dynamics of the hot donor molecules are characterized by measuring the nascent energy partitioning in scattered $H_2O(000)$ molecules and the absolute rates for energy transfer.

Transient IR absorption signals for appearance of a single rotational state of $H_2O(000)$ following collisions with hot donors are shown in Figure 1. IR intensities measured at t=1 μs following the UV pulse correspond to populations of individual H_2O states that result primarily from single collisions with hot donors, thus minimizing the effect of secondary collisions that relax the rotational and translational energies of the scattered

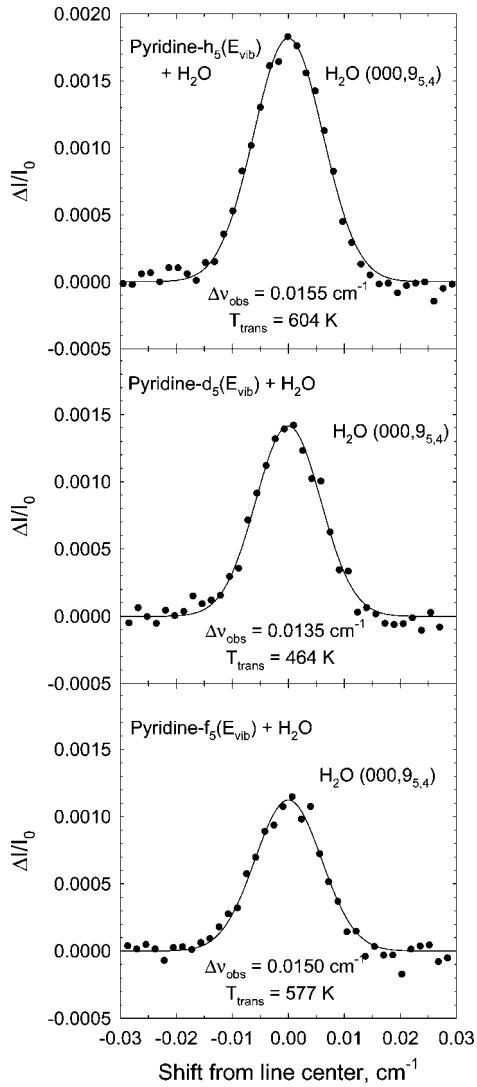

Figure 2. Transient absorption lineshapes for $H_2O(000,9_{5,4})$ collected at 1 μs following UV excitation of pyridine-h_5, pyridine-d_5, and pyridine-f_5. The data are shown as filled circles and are fit to a Gaussian function shown as a solid line.

$H_2O(000)$ molecules. The linearity of the transient signals in Figure 1 at early times following UV excitation of donor molecules is indicative of products resulting from single collisions between donor and water. Transient spectra were collected at t=1 μs as a function of probe laser wavelength to obtain Doppler broadened line profiles for scattered $H_2O(000)$, as shown in Figure 2. Nascent velocity distributions of the scattered molecules are obtained from transient line widths. Nascent populations are determined by the area under the transient line profile.

A number of improvements have been made in the new spectrometer to increase the quality of the transient absorption data. Improvements in IR power, beam alignment and detector sensitivity have resulted in a 5-fold increase in signal-to-noise levels of transient IR absorption measurements and a 3-fold decrease in the detector response time. The new spectroscopic method for measuring total cell pressure gives a more accurate measure of the time between collisions. Together these improvements have led to transient absorption signals (Figure 1) that are of higher quality and are more linear with respect to time than those in the original pyridine-h_5:H_2O study.[19]

In the next section we present new results for pyridine-h_5:H_2O collisions and compare them with the original data. We find that the energy transfer data from the two studies are consistent (with overlapping error bars) but the new energy gain profiles for rotation and translation of water are slightly larger than the original data. We attribute the difference in the pyridine-h_5:H_2O results to the influence in the original experiments of secondary collisions that relax the scattered water molecules. Based on our new method of measuring pressure, we estimate that the original data was collected at a pressure that was ~50% higher than reported, which leads to a 67% drop in the collision time from 2.5 to 1.6 μs. Previous transient measurements made at t = 1 μs are therefore likely to be affected by secondary collisions. In the current study, we compare data for the three donors that were collected on the new instrument under similar conditions of pressure and laser power where the influence of secondary collisions is reduced.

Results and Discussion

Here we present scattering data for large ΔE-collisions of pyridine-h_5, pyridine-d_5, and pyridine-f_5 with H_2O. We find that the scattered water states with E_{rot} > 1000 cm^{-1} have energy gain profiles due to collisions with pyridine-h_5 and-d_5 that are quite similar. Collisions with pyridine-f_5 impart less energy to the scattered water molecules. These results are discussed in terms of differences in the intermolecular potential interactions, donor state density, and mode frequencies.

Dynamics of Scattered $H_2O(000)$

The nascent rotational distribution of $H_2O(000)$ molecules scattered from the pyridine donors was determined by measuring the early time population changes of H_2O rotational states with E_{rot}=1000−1800 cm^{-1}. The rotational distribution for each donor:water pair was measured at t=1 μs following donor excitation and is shown in Figure 3a. Each data point is the average of at least 3 measurements of an individual water state. Each data set was fit to a Boltzmann distribution with a rotational temperature. The distribution of scattered water from pyridine-h_5 was measured to be T_{rot} = 890 ± 150 K. This result is slightly larger than, but within error of, our previous result of T_{rot} = 770 ± 80 K.[19] For collisions of water with pyridine-d_5, the scattered $H_2O(000)$ has a rotational temperature of T_{rot} = 890 ± 90 K, which is similar to the result for pyridine-h_5:H_2O. Less rotational energy is imparted to the high-J states of water in collisions with pyridine-f_5 where the rotational temperature of scattered water is T_{rot} = 530 ± 55 K.

For collisions that result in $H_2O(000)$ scattered into states with E_{rot} = 1000−1800 cm^{-1}, we estimate the average amount of donor vibrational energy that is converted into water rotation using $\langle \Delta E_{rot} \rangle = 3/2 k_B(T_{rot} - T_0)$ and T_0 = 298 K. In collisions with pyridine-h_5 and -d_5, the average change in water's rotational energy is $\langle \Delta E_{rot} \rangle \approx 610$ cm^{-1}. Much less energy goes into water rotation in collisions with pyridine-f_5 where $\langle \Delta E_{rot} \rangle \approx 240$ cm^{-1}.

The nascent translational energy distributions are similar for the large-ΔE collisions of water with pyridine-h_5, -d_5, and -f_5. Translational energy distributions were obtained from Doppler-broadened line widths of H_2O transitions after single collisions with highly vibrationally excited donors. Doppler-broadened line profiles (Figure 2) for individual water states measured at t = 1 μs after donor excitation were fit using a two-parameter Gaussian function to extract the full-width-half-maximum line width $\Delta\nu_{obs}$ and the intensity at line center. The nascent line widths and translational temperatures (in both the laboratory frame and the center-of-mass frame) are listed in Table 1 for a number of scattered water states with E_{rot} > 1000 cm^{-1}. The center-of-mass translational temperatures T_{rel} are a measure of

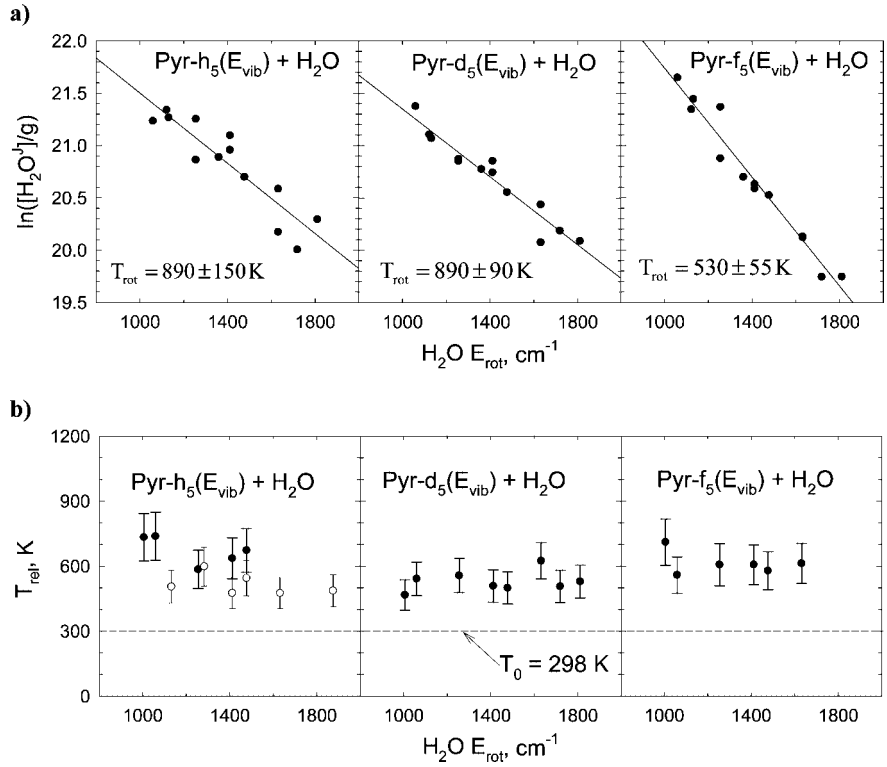

Figure 3. (a) Nascent distribution of $H_2O(000)$ rotational states after single collisions with pyridine-h_5, pyridine-d_5, and pyridine-f_5. Data are collected at 1 μs following donor excitation. Each point represents an average of three independent measurements. (b) Center of mass translational temperatures for pyridine-h_5:H_2O, pyridine-d_5:H_2O, and pyridine-f_5:H_2O shown as a function of H_2O rotational energy following collisional energy transfer. The open circles for pyridine-h_5:H_2O are taken from ref 19.

the recoil velocity distribution in the scattered molecules and have values that range from $T_{rel} = 467 \pm 70$ K to 738 ± 111 K. Values of T_{rel} are plotted as a function of water rotational energy in Figure 3b. The new results for pyridine-h_5 are slightly higher than, but within error of, our previous results which are shown as open circles in Figure 3b for comparison. The translational energy distributions for the three donors are similar and there is no clear dependence on the water rotational state. The lack of rotational dependence for T_{rel} appears to be a common feature in collisions of water with highly excited molecules and has been observed for both H_2O and HOD.[8,9,19]

Absolute rate constants (k_2^J in Eq. 1) for energy gain in individual water states were determined for each donor molecule to establish the importance of vibration-to-rotation/translation (V→RT) energy transfer. State-specific rate constants are provided as Supporting Information. Energy gain rate constants for individual H_2O states between $E_{rot} = 1000$ and 1800 cm^{-1} were summed to yield integrated rate constants k_2^{int} that are listed in Table 2 for each donor:water pair. These rates correspond to the subset of V→RT collisions that have large ΔE values. Determining the total rate that accounts for all V→RT collisions requires information about the low energy water states with $E_{rot} < 1000$ cm^{-1}, which is not currently available. Extrapolating the T_{rot} values for large-ΔE collisions to low-energy water states leads to an estimate of total V→RT energy transfer rates that are just slightly larger than the Lennard-Jones collision rates. This suggests that most quenching collisions involve the V→RT pathway and that V→RT energy transfer occurs on essentially every collision. These values are listed in Table 2. As a cross check we measured the rate of vibration-to-vibration (V→V) energy transfer for pyridine-f_5:H_2O collisions and find that excitation of the bending mode of water occurs at a rate that is only ~2% of the Lennard−Jones collision rate. Energy transfer to the higher frequency stretching modes of water was not observed.

Role of Donor Vibrational Mode Frequencies. Our state-resolved scattering measurements provide insight into the dynamics of large-ΔE collisions in molecules that have preferential hydrogen bonding interactions with water. We find that the scattering dynamics for water with pyridine-h_5 and with pyridine-d_5 are essentially the same. In collisions with pyridine-f_5, however, we observe a substantial decrease in the rotational energy of the scattered water molecules. A number of factors may explain why water gains more rotational energy in collisions with pyridine-h_5 and -d_5 than with pyridine-f_5. One factor could be the differences in the vibrational frequencies of the donor molecules which are affected by the reduced mass and the force constant of the oscillators. For these donors the effective reduced mass of the C−X bond decreases from $\mu = 1$ amu when X is H, to $\mu = 2$ amu when X is D and $\mu \approx 17$ amu when X is F, leading to a reduction in vibrational frequencies as the atom X becomes more massive. For example, the C−X stretch frequencies are ~3050 cm^{-1} for pyridine-h_5, ~2270 cm^{-1} for pyridine-d_5 and ~1550 cm^{-1} for pyridine-f_5.[26,27] The out-of-plane-bending modes and other low frequency modes are also affected by the mass of X and the oscillator force constant. The low frequency modes of pyridine-h_5, -d_5 and -f_5 are in the range of $\nu \approx$ 390−990, 340−820, and 170−650 cm^{-1}, respectively.[26,27]

A number of experimental and theoretical studies indicate that the low frequency modes of highly excited molecules are the most relevant modes for collisional energy transfer.[28–30] Based on this, we might expect that collisions with pyridine-f_5 will impart larger amounts of energy to the scattered water molecules, which is not observed in our measurements. In addition, if donor vibrational frequencies were influencing the

TABLE 1: Doppler-Broadened Linewidths and Translational Temperatures for Strong Collisions of $H_2O(000)$ with Vibrationally Excited Pyridine-h_5, Pyridine-d_5 and Pyridine-f_5

		pyridine-h_5 + H_2O		
$J_{Ka,Kc}$	E_{rot}, cm^{-1}	$\Delta\nu_{obs}$, cm^{-1}[a]	T_{trans}(lab),K[b]	T_{rel}, K[c]
$8_{3,6}$	1006.1160	0.0163	652 ± 98	733 ± 110
$7_{5,3}$	1059.6470	0.0161	656 ± 98	738 ± 111
$8_{5,4}$	1255.1670	0.0144	532 ± 80	585 ± 88
$8_{6,2}$	1411.6418	0.0150	574 ± 86	636 ± 95
$9_{5,4}$	1477.2970	0.0155	604 ± 91	673 ± 101
		pyridine-d_5 + H_2O		
$J_{Ka,Kc}$	E_{rot}, cm^{-1}	$\Delta\nu_{obs}$, cm^{-1}[a]	T_{trans}(lab),K[b]	T_{rel}, K[c]
$8_{3,6}$	1006.1160	0.0134	437 ± 65	467 ± 70
$7_{5,3}$	1059.6470	0.0140	499 ± 71	542 ± 77
$8_{5,4}$	1255.1670	0.0142	511 ± 72	557 ± 79
$8_{6,2}$	1411.6418	0.0136	472 ± 69	509 ± 75
$9_{5,4}$	1477.2970	0.0135	464 ± 69	500 ± 74
$10_{5,6}$	1718.7188	0.0149	567 ± 76	625 ± 84
$9_{7,2}$	1810.5879	0.0135	470 ± 70	507 ± 75
		pyridine-f_5 + H_2O		
$J_{Ka,Kc}$	E_{rot}, cm^{-1}	$\Delta\nu_{obs}$, cm^{-1}[a]	T_{trans}(lab),K[b]	T_{rel}, K[c]
$8_{3,6}$	1006.1160	0.0166	672 ± 101	711 ± 107
$7_{5,3}$	1059.6470	0.0144	534 ± 80	559 ± 84
$8_{5,4}$	1255.1670	0.0151	578 ± 87	607 ± 91
$9_{5,4}$	1477.2970	0.0150	577 ± 87	607 ± 91
$9_{6,3}$	1631.3831	0.0147	552 ± 83	579 ± 87

[a] The full width at half-maximum line width from fitting the t = 1 μs transient line profile to a Gaussian function (Figure 2). The uncertainty in line width measurements is ±0.001 cm^{-1}. [b] The laboratory frame translational temperature is found using $T_{trans}(lab) = (mc^2/8k_B \ln 2)(\Delta\nu_{obs}/\nu_0)^2$ where m is the mass of H_2O, c is the speed of light, k_B is Boltzmann's constant, ν_0 is the IR transition frequency and $\Delta\nu_{obs}$ is the nascent Doppler-broadened line width. [c] The center of mass translational temperature for an isotropic distribution of scattered molecules is found using $T_{rel} = T_{trans}(lab) + (T_{trans}(lab) - T_0) \times (m_{H_2O}/m_{donor})$ where T_0 = 298 K is the precollision temperature and donor = pyridine-h_5, pyridine-d_5 or pyridine-f_5.

TABLE 2: Comparison of Integrated Energy Transfer Rates (k_2^{int}), Total Collision Rates, and Lennard−Jones Collision Rates

donor molecules	k_2^{int} 10^{-10} cm^3 $molecule^{-1}$ s^{-1}	$k_{TOT} = \sum_{all\ J} k_2^J$ 10^{-10} cm^3 $molecule^{-1}$ s^{-1}	k_{LJ} 10^{-10} cm^3 $molecule^{-1}$ s^{-1}
H_2O E_{rot} range	1000 − 1800 cm^{-1}	0 − 3000 cm^{-1}	
pyridine-h_5 [a]	1.66 ± 0.42	6.91 ± 1.73	6.15[b]
pyridine-d_5	1.75 ± 0.44	7.28 ± 1.82	6.12[b]
pyridine-f_5	1.36 ± 0.34	10.7 ± 3.22	6.44[b]

[a] Rates for pyridine-h_5 quenching were determined using translational and rotational temperatures from this work. [b] Lennard−Jones collision rates were calculated using the following parameters: for pyridine-h_5 and pyridine-d_5, ε = 5.25 Å and σ = 465 K; for pyridine-f_5, ε = 5.69 Å and σ = 438 K. ε and σ values were determined from critical constants for C_6H_6, C_6H_5F, and pyridine-h_5.[39]

large-ΔE collisions, we would expect to see differences between the $-h_5$ and $-d_5$ donors, which are not observed as well. Our result is consistent with other studies showing that deuteration of highly vibrationally excited donor molecules has little effect on overall energy transfer behavior.[28,31] Of course, the measurements in the current study are focused on the dynamics of the high energy tail of the V-RT pathway and do not provide information about small-ΔE collisions. It may be that the small-ΔE collisions are sensitive to differences in donor vibrational frequencies.

Role of Donor State Density. Collisional energy transfer of highly vibrationally excited molecules is known to be affected by changes in the vibrational state density of the donor. Increasing donor state density tends to enhance energy transfer probabilities. High resolution IR studies have shown that the curvature of the high energy tail of the energy transfer distribution function correlates with the energy dependence of the donor state density for collisions in a CO_2 bath.[32] A related dependence on state-density has been seen in the rotational distributions of scattered water molecules in collisions with highly excited donors.[20] The GRETCHEN model for large-ΔE collisions, based on Fermi's Golden Rule, outlines this state density dependence.[20,32] Statistical theories inherently include state density in collisional energy transfer, and recent developments in the Partially Ergodic Collision Theory of Nordholm and co-workers consider subspaces of state density that give excellent agreement with the KCSI experiments of Luther and co-workers.[33–35]

The donor molecules studied here have state densities at E = 38 000 cm^{-1} of $\rho = 6.24 \times 10^{13}$ states/cm^{-1} for pyridine-h_5, $\rho = 1.90 \times 10^{15}$ for pyridine-d_5 and 1.48×10^{20} for pyridine-f_5. The state density of the fluorinated donor has the strongest energy dependence of these donors, and we observe that pyridine-f_5 imparts the smallest amount of rotational energy to H_2O. The rotational energy gain profiles for water following collisions with pyridine-h_5, pyridine-d_5, and pyridine-f_5 agree reasonably well with predictions from the GRETCHEN model, but there is some discrepancy for pyridine-h_5 and -d_5. The GRETCHEN model predicts that T_{rot} for pyridine-d_5 collisions should be slightly less than for pyridine-h_5, but this is not observed. However the state density difference in these donors is not very large and the difference in their energy dependence is even smaller, so differences in the scattering results may be within our experimental uncertainty. It is interesting that if both the rotational energy and translational energy exchanges are considered, the correlation of water energy transfer data and donor state density energy dependence washes out. The Doppler broadened line widths for water do not increase as a function of rotational state, giving similar translational energy distributions to each rotational state of H_2O. This tends to flatten out the overall energy transfer distribution function for large-ΔE collisions. This situation is quite different from CO_2 collisions, where extensive line broadening is observed for scattering to high rotational states.[36,37] It may be that for strongly interacting collision partners, such as aromatic donors with water, the attractive interactions outweigh the impulsive nature of the collisions leading to different state density effects. The fact that we do not observe differences in the scattering dynamics of H_2O from pyridine-h_5 and pyridine-d_5, but do see differences for collisions with pyridine-f_5, supports the idea that electrostatic interactions are important in the large-ΔE collisions of water.

Preferential Hydrogen Bonding Effects. In this section we consider how differences in the intermolecular potential energy surfaces of water with pyridine-h_5, -d_5 and -f_5 might affect the types of motions that water undergoes in collisions with these highly excited donors. The interaction of water with each of these donors has minima in the σ- and π-hydrogen bonding orientations. It is possible that water

moves from one energy minimum to the other during collisions and that this type of motion influences the partitioning of energy in the scattered water molecules. Shuttling motion of water between different hydrogen bonding sites has been observed for stable complexes of transformaniline in experiments by Zwier and co-workers.[38] Motion of water from a π-configuration to a σ-configuration (and vice versa) is likely to promote rotational energy in the scattered bath molecules. If this type of directed motion of water occurs in collisions with highly excited pyridine donors, then donors for which water can more easily move between σ- and π-sites are expected to impart more rotational energy to water.

For pyridine-h_5 and pyridine-d_5, the π-complex with water is likely to have a minimum energy configuration that is roughly that of benzene$-H_2O$, with the hydrogen atoms of water directed toward the electron-rich π-cloud.[10,15] Similarly, π-complexes of pyridine-f_5 are most likely similar in structure to those of $C_6F_6-H_2O$, with the hydrogen atoms of water directed away from the π-cloud.[10] For the C_6H_6 complex, water is $\sim$3 Å from the π -cloud as compared to a distance of $\sim$4 Å in $H_2O-C_6F_6$. The interaction energies of these complexes are similar, both $\sim$2 kcal/mol. In collisions of the type we have studied, it is unlikely that multiple shuttling events occur between the σ- and π- sites, just as it is unlikely that stable complexes are formed. It is possible however that the ease with which water moves between σ- and π- sites on the donors affects the amount of rotational energy it gains during collisions. Directed movement of water between σ- and π-sites on pyridine-h_5 and pyridine-d_5 should be easier than for pyridine-f_5 given the proximity of the hydrogen atoms to the aromatic ring and the simpler motion required to move between σ- and π-orientations. The reversed orientation of water in the fluorinated complex is likely to hinder its ability to move between the σ- and π- orientations. Taken together, this situation should impart less rotational energy to water and may be one reason that water is scattered from pyridine-f_5 with less rotational energy. Of course, collisions occur over a wide range of initial impact parameters and orientations and the σ-π hydrogen bonding swapping mechanism discussed here describes just one type of collisional encounter. Nevertheless, the σ- and π-hydrogen bonded orientations are the global minima in the intermolecular potential energy surface of water with pyridine. The ease with which water can move between these sites, and the extent to which these forces direct its motion, are likely to influence molecular collisions. The scattering data are consistent with the type of torque-inducing interactions described above. Computer simulations of collisions between highly vibrationally excited pyridine-h_5, -d_5, and -f_5 with water are expected to provide insight into the importance of this phenomenon in the collisional quenching of highly excited molecules with water.

Conclusions

The state-resolved energy gain profiles of scattered $H_2O(000)$ molecules with $E_{rot} > 1000$ cm^{-1} are reported for quenching collisions with highly vibrationally excited pyridine-h_5, pyridine-d_5, and pyridine-f_5 ($E \approx 38\,000$ cm^{-1}). Our results show that water molecules scattered from pyridine-h_5 and -d_5 have similar rotational distributions of $T_{rot} = 890$ K. Collisions with pyridine-f_5 scatter water with less rotational energy and a rotational temperature of $T_{rot} = 530$ K. The distributions of recoil velocity are similar for the three donor molecules and have center-of-mass translational temperatures of 400−700 K. The energy transfer rates are similar for the three donors and indicate that the V-RT pathway is the dominant relaxation route for these donors with water. Our results show that energy transfer into the bending vibrational mode of water accounts for only $\sim$2% of all collisions. Differences in the vibrational frequencies of the three donor molecules do not appear to explain the observed reduction in rotational energy of the scattered water molecules when pyridine-f_5 is the donor molecule. The experimental results are consistent with differences in state density of the highly excited donor molecules but the correlation of the energy transfer distribution with state density energy dependence is less than ideal and does not account for similarities in scattering data of the pyridine-h_5 and -d_5 donors. A third explanation is that motion between σ-and π-hydrogen bonding sites on the highly excited donors influences the extent to which water gains large amounts of rotational energy through a torque-inducing mechanism. This motion will be the same for pyridine-h_5 and -d_5 based on the most stable π-configurations of aromatic species with hydrogen atoms. The strong electronegativity of fluorine atoms in pyridine-f_5 reverses water's orientation for the most stable π-configuration. This orientation is likely to hinder motion between the σ- and π-sites of the fluorinated donor and lead to a reduction in the rotational energy of the scattered water molecules. This torque-inducing mechanism is consistent with our experimental observations. The extent to which this type of motion occurs on pyridine$-H_2O$ collisions can be investigated in the future using molecular dynamics simulations.

Acknowledgment. The authors acknowledge support from the Department of Energy, Basic Energy Science (DE-FG-02-06ER15761) with equipment from the National Science Foundation (CHE-0552663). J. McQueeney is thanked for mechanical assistance.

Supporting Information Available: A description of the spectroscopically calibrated manometer pressure measurements. Tabulated state-specific rate constants for appearance of $H_2O(000,J_{KaKc})$ following collisions with highly vibrationally excited pyridine-h_5, -d_5, and -f_5. This material is available free of charge via the Internet at http://pubs.acs.org.

References and Notes

(1) Guckian, K. M.; Schweitzer, B. A.; Ren, R. X. F.; Sheils, C. J.; Tahmassebi, D. C.; Kool, E. T. *J. Am. Chem. Soc.* **2000**, *122*, 2213.
(2) Hunter, C. A. *Chem. Soc. Rev.* **1994**, *23*, 101.
(3) Coates, G. W.; Dunn, A. R.; Henling, L. M.; Dougherty, D. A.; Grubbs, R. H. *Angew. Chem., Int. Ed. Engl.* **1997**, *36*, 248.
(4) Nadykto, A. B.; Yu, F. Q. *Chem. Phys. Lett.* **2007**, *435*, 14.
(5) Aloisio, S.; Hintze, P. E.; Vaida, V. *J. Phys. Chem. A* **2002**, *106*, 363.
(6) Smith, I. W. M.; Ravishankara, A. R. *J. Phys. Chem. A* **2002**, *106*, 4798.
(7) Caminati, W.; Favero, L. B.; Favero, P. G.; Maris, A.; Melandri, S. *Angew. Chem., Int. Ed.* **1998**, *37*, 792.
(8) Havey, D. K.; Liu, Q.; Li, Z.; Elioff, M.; Mullin, A. S. *J. Phys. Chem. A* **2007**, *111*, 13321.
(9) Havey, D. K.; Liu, Q.; Li, Z.; Elioff, M.; Fang, M.; Neudel, J.; Mullin, A. S. *J. Phys. Chem. A.* **2007**, *111*, 2458.
(10) Danten, Y.; Tassaing, T.; Besnard, M. *J. Phys. Chem. A* **1999**, *103*, 3530.
(11) Alkorta, I.; Rozas, I.; Elguero, J. *J. Fluorine Chem.* **2000**, *101*, 233.
(12) Rozas, I.; Alkorta, I.; Elguero, J. *J. Phys. Chem. A* **1997**, *101*, 9457.
(13) Furutaka, S.; Ikawa, S. *J. Chem. Phys.* **2002**, *117*, 751.
(14) Atwood, J. L.; Hamada, F.; Robinson, K. D.; Orr, G. W.; Vincent, R. L. *Nature* **1991**, *349*, 683.
(15) Suzuki, S.; Green, P. G.; Bumgarner, R. E.; Dasgupta, S.; Goddard, W. A.; Blake, G. A. *Science* **1992**, *257*, 942.
(16) Engdahl, A.; Nelander, B. *J. Phys. Chem.* **1987**, *91*, 2253.
(17) Gotch, A. J.; Zwier, T. S. *J. Chem. Phys.* **1992**, *96*, 3388.
(18) Wormald, C. J.; Wurzberger, B. *Phys. Chem. Chem. Phys.* **2000**, *2*, 5133.

(19) Elioff, M. S.; Fraelich, M.; Sansom, R. L.; Mullin, A. S. *J. Chem. Phys.* **1999**, *111*, 3517.
(20) Elioff, M. S.; Fang, M.; Mullin, A. S. *J. Chem. Phys.* **2001**, *115*, 6990.
(21) Fraelich, M.; Elioff, M. S.; Mullin, A. S. *J. Phys. Chem. A* **1998**, *102*, 9761.
(22) Villa, E.; Amirav, A.; Lim, E. C. *J. Phys. Chem.* **1988**, *92*, 5393.
(23) Yamazaki, I.; Murao, T.; Yamanaka, T.; Yoshihara, K. *Faraday Discuss.* **1983**, 395.
(24) Alani, K.; Phillips, D. *J. Phys. Chem.* **1970**, *74*, 4046.
(25) Yamazaki, I.; Sushida, K.; Baba, H. *J. Chem. Phys.* **1979**, *71*, 381.
(26) Wong, K. N.; Colson, S. D. *J. Mol. Spectrosc.* **1984**, *104*, 129.
(27) Long, D. A.; Steele, D. *Spec. Acta* **1963**, *19*, 1791.
(28) Toselli, B. M.; Barker, J. R. *J. Chem. Phys.* **1992**, *97*, 1809.
(29) Mitchell, D. G.; Johnson, A. M.; Johnson, J. A.; Judd, K. A.; Kim, K.; Mayhew, M.; Powell, A. L.; Sevy, E. T. *J. Phys. Chem. A* **2008**, *111*, 13330.
(30) Clary, D. C.; Gilbert, R. G.; Bernshtein, V.; Oref, I. *Faraday Discuss.* **1995**, 423.
(31) Wu, F.; Weisman, R. B. *J. Chem. Phys.* **1999**, *110*, 5047.
(32) Park, J.; Shum, L.; Lemoff, A. S.; Werner, K.; Mullin, A. S. *J. Chem. Phys.* **2002**, *117*, 5221.
(33) Lenzer, T.; Luther, K.; Nilsson, D.; Nordholm, S. *J. Phys. Chem. B* **2005**, *109*, 8325.
(34) Nilsson, D.; Nordholm, S. *J. Chem. Phys.* **2003**, *119*, 11212.
(35) Nilsson, D.; Nordholm, S. *J. Phys. Chem. A* **2006**, *110*, 3289.
(36) Mullin, A. S.; Michaels, C. A.; Flynn, G. W. *J. Chem. Phys.* **1995**, *102*, 6032.
(37) Wall, M. C.; Mullin, A. S. *J. Chem. Phys.* **1998**, *108*, 9658.
(38) Clarkson, J. R.; Baquero, E.; Shubert, V. A.; Myshakin, E. M.; Jordan, K. D.; Zwier, T. S. *Science* **2005**, *307*, 1443.
(39) Anon CRC Handbook of Chemistry and Physics: A Ready-Reference of Chemical and Physical Data, 85th ed, Edited by David R. Lide, 2005, Sec. 6−56, 6−59, 6−60.

JP802326T